

Improvements to the ICP Algorithm for Shape Registration in Manufacturing

Tsz-Ho Kwok*, and Kai Tang

Department of Mechanical and Aerospace Engineering, The Hong Kong University of Science and Technology

Iterative Closest Point (ICP) is a popular algorithm used for shape registration while conducting inspection during a production process. A crucial key to the success of ICP is the choice of point selection method. While point selection can be customized for a particular application using its prior knowledge, *Normal-Space Sampling* is commonly used when normal vectors are available. Normal-based approach can be further improved by stability analysis – called covariance sampling. The stability analysis should be accurate to ensure the correctness of covariance sampling. In this paper, we go deep into the details of covariance sampling, and propose a few improvements for stability analysis. We theoretically and experimentally show that these improvements are necessary for further success in covariance sampling. Experimental results show that the proposed method is more efficient and robust for the ICP algorithm.

Keywords: ICP, shape registration, inspection, point selection, stability analysis, kinematic.

1 Introduction

Registration is a process to align different datasets in a same coordinate system. It is a fundamental task in many applications of computer vision, pattern recognition, computer graphics, medical imaging, etc. In manufacturing, to register a point cloud scanned from a fabricated part with a 3D Computer-Aided Design (CAD) model is an important process for quality control and inspection. Lately, the layer-based additive manufacturing (AM) method [23] is also advancing to 6-axis AM [17], which requires an accurate registration. It is also referred to as *scene-to-model registration* that finds an optimal rigid transformation (six degrees of freedom in translations and rotations) to align one dataset (model) to another (scene). “Model” and “scene” are the aliases for two datasets, where “scene” stands for the static one and “model” stands for the moving one. The most popular fine registration method is the *Iterative Closest Point* (ICP) algorithm [1]. ICP has many different elements, which can be summarized into one or more of these categories [14]: point selection, point matching, pair weighting, outlier removal, error metric, and energy minimization. In general, these steps are applied sequentially in an ICP process, but

it is not a must to perform all these steps; each step is performed only if necessary. In this paper, we mainly focus on the category of point selection. Point selection is usually performed for the sake of convergence and computational complexity, or sometimes for outlier removal. This is because indiscriminately using all the points for registration will inordinately slow the ICP convergence, find a wrong pose, or even make ICP diverge. In the ideal case, it is desirable to use the minimum number of points for the same level of accuracy. It is natural to look for good strategies in point selection based on different prior knowledges. For instance, uniform sampling [20], random sampling [11], sampling on intensity or color [22], sampling on normal-space [14], etc. Normal is available in most of applications, and *Normal-Space Sampling* (NSS) is to choose a certain number of points such that the distribution of normals among selected points is as-large-as-possible. NSS is known to perform much better than uniform sampling [14], and thus it is commonly used in practice. The normal information can be further analyzed to find a set of points that can better constrain the transformation. Gelfand et al. [6] proposed the stability analysis, and based on that, they developed the covariance sampling for ICP. Our study is motivated by their work, and we further confirm that the accuracy of the stability analysis is very important for covariance sampling. We propose several key improvements to the stability analysis that help increase the accuracy (often substantially), along with their theoretic proof and experimental data.

On the other hand, some approaches rely on different local shape descriptors to select the points that have singular descriptor values for registration [7], and expect that these singular points can uniquely define the transformation between the input datasets. Although using rare points may be a good strategy for registration, not every model has distinguishable features, especially when only partial registration can be done (e.g., unfinished workpiece in machining). For example, the surface of a blade model is featureless. Even the sharp edges of the blade are not good candidates. This is because the leading or trailing edge have extremely small dimensions, and thus the machining and measuring errors are relatively much higher than at other places, which makes the edges not reliable in registration. We will show in this paper that the improved stability analysis can be used as a quantitative measurement to check if the selected points are suffi-

*Corresponding author: tom.thkwok@gmail.com

cient for registration. The stability of registration is defined as the error introduced when the object performs an infinitesimal motion from the desired location. In other words, large registration errors will be introduced when the object is not placed exactly in the desired location; therefore, the whole registration process can be converged quickly and become more stable.

In this paper, we present several improvements for stability analysis and covariance sampling in defining the rotation center, point extraction, and torque normalization. We summarize the contributions as:

1. Rotation center is commonly set as the center of mass; however, it is not always valid. We develop an axis/center-iteration algorithm to find the correct rotation center, which is a nonlinear problem.
2. The selected point set is updated throughout the point extraction process, so the principle axes of the motion are changed too, which is another nonlinear optimization problem. We develop an addition/reduction-iteration algorithm to extract an elite point set.
3. Normalization between the force and torque is not well-understood, and there are different ways for the normalization. We study this problem and experimentally induce the correct normalization of torque for ICP applications.

Our introduced methods enable a quantitative measurement to evaluate the stability of the selected points. We can reduce the number of points to achieve the same level of accuracy by finding out a set of points that can provide the needed stability.

In the rest of this paper, we will first give a brief review of related works, in Section 2. After that, Section 3 will introduce the basic details of ICP, as well as the idea of stability analysis. Section 4 presents our proposed improvements for stability analysis. Experimental results are given in Section 5. Finally, the paper is concluded in Section 6.

2 Related Works

There is quite a large amount of research work in surface registration (e.g., [10]). For a detailed review, readers are referred to a thorough survey paper on surface registration [15]. Among all, the *Iterative Closest Point* (ICP) algorithm [1] is a widely used method for aligning different parts of an object. Pottmann and Leopoldseider [13] proposed the *Squared Distance Minimization* (SDM) for ICP in minimizing the error between different datasets. The SDM technique has variants in different orders: the zero-order approximation of surface distance – *Point Distance* (PD) – uses the closest point as the target for fitting [1]; the first-order – *Tangent Distance* (TD) – measures the fitting error by using the projection on the tangent plane as the target [3]; the second-order – *Square Distance* (SD) – uses the curvature information to approximate the local shape [12]. Higher order can give better approximation, but the performance of SD is the same as TD when the datasets are close to each other [21]. How-

ever, the quality of alignment obtained by ICP still heavily depends on choosing good pairs of corresponding points in the two datasets. Gelfand et al. [6] pointed out that if too many points are chosen from featureless regions of the data, the algorithm could fail. They proposed a geometrically stable ICP by choosing samples that constrain unstable transformation to minimize the uncertainty in registration. The point selection in their stable ICP is based on the stability analysis, or slippage analysis [5]. The basic idea is that the position of a feature (called slippage feature [2]) should be uniquely defined within a local neighborhood so that the feature correspondence is locally well defined. Their approach is valuable because it uses fewer points but provides better convergence than the Normal-Space Sampling [14] without requiring more information. Therefore, in this paper we provide a few more improvements, aiming to increase the usage and the impact of stability analysis.

Besides, there are also research results that use local shape descriptors to select feature points for registration; for example, curvature map [4], integral volume descriptor [7], intrinsic wave descriptor [19], Heat Kernel Signature (HKS) [18], 3D-SIFT [8] (see [9] for a survey). Based on different local shape descriptors, most of the existing methods select the points that have rare or unique descriptor values for registration, and expect that these rare points can uniquely define the transformation. Song et al. [16] detected saliency information for each scan, and employed Markov random field (MRF) to partition scans into salient and non-salient regions. The rare points are then selected from the salient regions. However, indiscriminately using all the rare points could lead to too many redundancies for ICP. On the other hand, there would be not enough rare points if the object has few or even no feature regions. In principle, seven points are sufficient to uniquely define the geometric placement. However, extra points are desired to reduce the demand of accuracy from each point, and thus increase the stability and robustness for the whole system. In this paper, we study how to find the minimum number of points that can achieve the demanded level of stability.

3 Stability Analysis for ICP

In this section, we briefly describe the basic idea and formulation of the stability analysis proposed by Gelfand et al. [6]. Without loss of generality, we assume that the global (or rough) registration is already available, and we focus on solving the fine registration by the Iterative Closest Point (ICP) algorithm. Let $P = \{\mathbf{p}_1, \mathbf{p}_2, \dots, \mathbf{p}_n\}$ be the points on the model, and S be the scene. The goal of the registration algorithm is to find a rigid body transformation that best aligns the point cloud P to match the scene S . The procedure of ICP is to select k feature points from P , and minimize the following energy function:

$$E_{ICP} = \sum_{i=1}^k d^2(\mathbf{R}\mathbf{p}_i + \mathbf{t}, S), \quad (1)$$

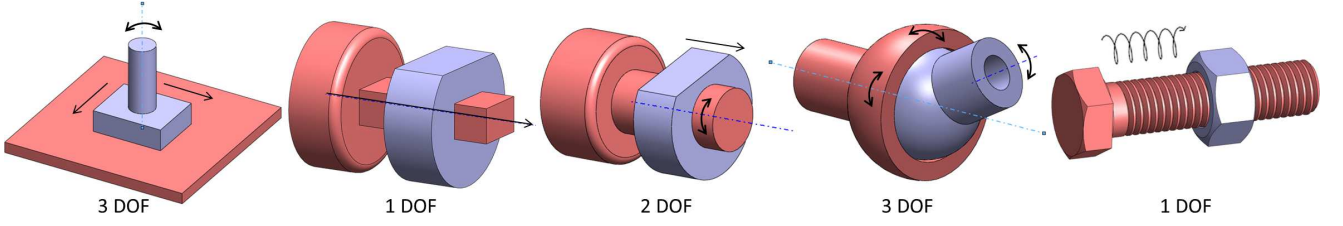


Fig. 1. The contact surfaces of these mechanical parts are not completely constrained, i.e., they have certain degrees of freedom (DOF).

where \mathbf{R} is the rotation matrix, \mathbf{t} is the translation vector, and d^2 is the squared distance function measuring from the transformed point \mathbf{p}_i to the surface S .

The optimal transform between P and S can be found by minimizing Eq.(1). The robustness of this optimization mainly depends on the stability of the energy function to the distance between the object's current placement and its desired placement. Inversely but equivalently, the stability of ICP can be defined as the amount of energy introduced in Eq.(1) when the object is moved away from the desired placement with an infinitesimal distance. This is because it represents the gradient (or the first derivative) of Eq.(1) at the optimal point, and we know that in the optimization theory a system converges faster if the gradient is larger. In the other words, the larger the gradient is, the more difficult for the system to leave its optimal solution, and hence more stable. Therefore, it is called the stability of ICP. Placing most of the points in the kinematic surfaces (e.g., the contact surfaces of the mechanical parts as shown in Fig.1) cannot help in registration, as they can freely move along the kinematic surfaces without introducing any energy. Therefore, we have to analyze the points to see if they constitute a kinematic surface.

The motion of a point at a particular time instance can be described as a twist $\delta\mathbf{w}$, which consists of a translation $\delta\mathbf{t}$ along a unique axis in wrench space and a rotation $\delta\mathbf{r}$ about that axis: $\delta\mathbf{w} = [\delta\mathbf{t} \ \delta\mathbf{r}]^\top \in \mathfrak{R}^6$, with $\delta\mathbf{t} = [t_x \ t_y \ t_z]^\top$, and $\delta\mathbf{r} = [r_x \ r_y \ r_z]^\top$. A wrench is a system of forces and moments acting on a rigid body that induces the twist, and the displacement of the point \mathbf{p}_i in Euclidean space is given by a vector $(\delta\mathbf{r} \times \mathbf{p}_i + \delta\mathbf{t})$. We can think of this as measuring the error induced when a point is leaving from its desired position. In such particular instant, the target point is assumed to be itself. Using Tangent Distance (TD) as the distance function d^2 , the ICP energy can be represented in terms of the twist by

$$E = \sum_{i=1}^k \|(\delta\mathbf{r} \times \mathbf{p}_i + \delta\mathbf{t}) \cdot \mathbf{n}_i\|^2, \quad (2)$$

where $\mathbf{n}_i = [n_x \ n_y \ n_z]^\top$ is the normal vector of \mathbf{p}_i . The unit normal force on a point \mathbf{p}_i in wrench space can be written as

$$\mathbf{u}_i = \begin{bmatrix} \mathbf{n}_i \\ \boldsymbol{\tau}_i \end{bmatrix} = \begin{bmatrix} \mathbf{n}_i \\ \mathbf{p}_i \times \mathbf{n}_i \end{bmatrix} \in \mathfrak{R}^6, \quad (3)$$

which is a unit force in the direction of \mathbf{n}_i and a unit moment along the axis $\boldsymbol{\tau}_i = \mathbf{p}_i \times \mathbf{n}_i = [\tau_x \ \tau_y \ \tau_z]^\top$. The stability of the

whole system is the minimum energy introduced by a twist in an arbitrary direction. To find out the axis for a twist that produces the least energy, we can take partial derivatives on E and set them to be zero. This yields a 6×6 linear equation system with respect to $\delta\mathbf{w} = [t_x \ t_y \ t_z \ r_x \ r_y \ r_z]^\top$ in the form of $\mathbf{H}\delta\mathbf{w} = 0$:

$$\mathbf{H} = \sum \begin{bmatrix} n_x n_x & n_x n_y & n_x n_z & n_x \tau_x & n_x \tau_y & n_x \tau_z \\ n_y n_x & n_y n_y & n_y n_z & n_y \tau_x & n_y \tau_y & n_y \tau_z \\ n_z n_x & n_z n_y & n_z n_z & n_z \tau_x & n_z \tau_y & n_z \tau_z \\ \tau_x n_x & \tau_x n_y & \tau_x n_z & \tau_x \tau_x & \tau_x \tau_y & \tau_x \tau_z \\ \tau_y n_x & \tau_y n_y & \tau_y n_z & \tau_y \tau_x & \tau_y \tau_y & \tau_y \tau_z \\ \tau_z n_x & \tau_z n_y & \tau_z n_z & \tau_z \tau_x & \tau_z \tau_y & \tau_z \tau_z \end{bmatrix}. \quad (4)$$

\mathbf{H} is the summation of Hessian matrices from each point (subscript i for each node is omitted in the above equation). The Hessian \mathbf{H} may not be of full rank, depending on the shape and the selected points. In this paper, we are interested in all the bases of the wrench space including those in the null spaces. The bases can be found by computing the eigenvalue decomposition $\mathbf{H} = \mathbf{Q}\mathbf{\Lambda}\mathbf{Q}^\top$, where $\mathbf{Q} = \{\mathbf{w}_1, \dots, \mathbf{w}_6\}$ consists of the bases (eigenvectors), and $\mathbf{\Lambda} = \{\lambda_1, \dots, \lambda_6\}$ gives the energies (eigenvalues) introduced by a unit normal wrench on the corresponding basis (sorted in ascending order). The eigenvalues actually indicate the stability along the corresponding eigenvectors. The smallest eigenvalue is thus the stability of the whole system.

4 Improvements for Stability Analysis

As pointed out in the previous section, the eigenvalues actually represent the stability of the system. Therefore, it is imperative for them to be correct. To ensure this correctness, several important improvements should be made. In this section, two nonlinear optimization problems – finding a correct rotation center and finding a good point selection – are addressed, and we will experimentally induce a correct normalization between the torque and force. They are crucial; because, if they are not correct, the stability of the system will be reported wrongly as high. For example, if the rotation center for a sphere is selected at a place other than the sphere center, even the smallest eigenvalue will not be zero as the sphere was supposed to be (more details will be given in the subsections). Therefore, the correctness is defined as the global optimum in the stability of the system, and the goal is to minimize the eigenvalues.

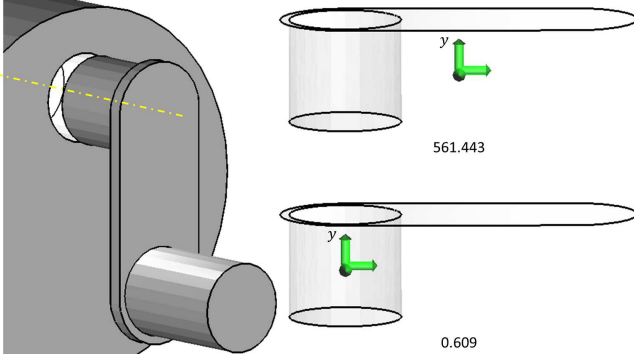


Fig. 2. These two parts are mechanically constrained (left), where their contact surface (right) is analyzed. (Top-right) Before optimizing the rotation center position (located at the intersection of the three rotation axes), the stability of the y-axis is reported as high. (Bottom-right) After updating the rotation center, the analysis gives a much lower stability for the y-axis.

4.1 Rotation Center

As rotation is a geometric operation turning around a center, the analysis can give a correct result only when a correct center is given. The rotational component in Eq.(2) can be rewritten as

$$E = \sum_{i=1}^k \|(\delta \mathbf{r} \times (\mathbf{p}_i^* - \mathbf{c}) + \delta \mathbf{t}) \cdot \mathbf{n}_i\|^2, \quad (5)$$

where $\mathbf{c} = [c_x \ c_y \ c_z]^\top$ is the rotation center, and $\mathbf{p}_i = \mathbf{p}_i^* - \mathbf{c}$ is assigned to distinguish the Euclidean position \mathbf{p}_i^* from the vector \mathbf{p}_i , with the center \mathbf{c} as the start point. Similar to *Principle Component Analysis* (PCA), most of the previous works assume the rotation center \mathbf{c} to be the center of mass of the model. By shifting the center of mass to the origin of the coordinate system, the rotation center \mathbf{c} is then the origin $(0, 0, 0)$. That is exactly the reason why the center is not seen in the equations. However, the center of mass is not always equivalent to the rotation center, e.g., the shape in Fig.2. We find that when the rotation center is not correctly given, the stability analysis could report erroneous information. Therefore, it is crucial for the rotation center to be correct.

Solving the rotation and its center altogether would be a highly nonlinear problem. In order to solve it efficiently, we separate and solve it in two phases. In the first phase, we fix the rotation center (\mathbf{c}) and solve for the rotation axis ($\delta \mathbf{r}$). In the second phase, the rotation axis is fixed while the rotation center is sought. These two phases are iteratively performed until the update in the position of the rotation center is less than a small value, e.g., 10^{-2} .

Axis Phase

Solving the linear equation system $\mathbf{H}\delta \mathbf{w} = \mathbf{0}$ discussed in Section 3 (i.e., Eq.(5)) gives all the bases of the motion. Remark that, \mathbf{p}_i should be updated with the rotation center \mathbf{c} in each step throughout the iterations. The surface's center of mass is used as the initial guess for center \mathbf{c} at the beginning. The results of this phase are the eigenvectors $\{\mathbf{w}_1, \dots, \mathbf{w}_6\}$,

and they are the bases used to compute a new center in the second phase.

Center Phase

The rotation axis is used to compute a new rotation center. By taking partial derivatives on Eq.(2), a linear equation system of $\mathbf{A}\mathbf{c} = \mathbf{b}$ can be obtained for each basis already computed in the axis phase, where

$$\mathbf{A}_1 = \sum (\delta \mathbf{r} \times \mathbf{n})(\delta \mathbf{r} \times \mathbf{n})^\top,$$

$$\mathbf{b}_1 = \sum (\delta \mathbf{r} \times \mathbf{n})(\mathbf{p}^* \cdot (\delta \mathbf{r} \times \mathbf{n}) - \delta \mathbf{t} \cdot \mathbf{n}).$$

One basis gives three equations, and six bases give eighteen equations. \mathbf{A} is not of full rank (i.e., $\text{rank}(\mathbf{A}) = \text{rank}(\mathbf{A}|\mathbf{b}) = 1$), and pure translation bases will give vanished equations, so the overall system can have multiple solutions. Without loss of generality, it can be solved by the Least Squares method consistently on the eighteen equations. Furthermore, in order not to be biased by the high error bases in the Least Squares solution, each equation of a basis is divided by the basis's eigenvalue. The result of this phase is a new position of rotation center, which is then the new input to the first phase in the next iteration.

Iterating these two phases eventually will lead to the optimal (or near-optimal) center. An example is shown in Fig.2. This figure shows two parts that are mechanically constrained, and they are rotated against each other around a rotation axis with a contact surface. Registration on this contact surface should be instable around the rotation axis. However, using the center of mass as the rotation center would wrongly give a high stability value (561.443) for the surface. After finding the optimal center, the analysis gives a correct result (now only 0.609).

4.2 Point Extraction

The ideal situation is that we can use the minimum number of points to get the same level of stability in registration. Recall that, solving Eq.(2) gives us six eigenvectors and eigenvalues, where the eigenvalues represent the stability in the corresponding eigenvectors. Based on the stability analysis on a given set of chosen points, Gelfand et al. [6] proposed a greedy algorithm to each time add a point with the largest energy in the most unconstrained eigenvector. Their idea is to equally constrain all eigenvectors, such that the total number of points is minimized. In their setup, the eigenvectors are kept the same throughout the whole process. Nevertheless, due to the reason that E in Eq.(2) and \mathbf{H} in Eq.(4) are the summations of energies and Hessian matrices for all the selected points, the eigenvectors obtained from \mathbf{H} do change when an individual point is added into or removed from the chosen point set. The situation is actually even more complicated, because a point that does not contribute much in

the current eigenvectors may contribute to the new eigenvectors. Therefore, the point extraction is actually a nonlinear optimization problem.

To handle this nonlinear optimization problem, again, we propose a two-phases algorithm to extract points. In the first phase, we add the high contributive points to the chosen point set, while in the second phase, we remove the low contributive points from the point set. Whenever the chosen point set is updated, the stability analysis is run to update the eigenvectors and eigenvalues. Therefore, these two nonlinear optimization problems are in a nested loop, with the point extraction in the outer loop, while the rotation center identification in the inner loop. It is worthwhile to mention that this process is fast. Although stability analysis is a time consuming process when it is running on a large point set, we start by adding points to the initial empty set, such that the whole process is dealing with only a small number of points which does not take much time.

Addition Phase

For the given eigenvectors $\{\mathbf{w}_1, \dots, \mathbf{w}_6\}$ of the chosen point set Φ (if $\Phi = \emptyset$, all the candidate points will be used to compute the eigenvectors), they are sorted according to the eigenvalues in the ascending order. Among all the candidate points, the one that has the largest value of $(\mathbf{u}_i \cdot \mathbf{w}_1)^2$ will be added to Φ . When the number of points in Φ is more than six (i.e., $|\Phi| > 6$), the eigenvectors are updated based on the current chosen point set.

Reduction Phase

The points added in the beginning may be no longer significant in the current eigenvectors. In order to keep an elite set, we go through a reduction phase when $|\Phi| > 20$ and for every n steps of additions. In this phase, $\frac{n}{4}$ points will be removed from Φ that have the smallest total sums of $(\mathbf{u}_i \cdot \mathbf{w}_k)^2$. We set $n = 10$ in our experiments.

We set the target for the stable situation to be when the energy E is greater than or equal to a minimum error of λ_{min} . In other words, all the eigenvalues must be at least λ_{min} , i.e., $(\lambda_1, \dots, \lambda_6 \geq \lambda_{min})$. The two phases are iterated until this target is achieved. If λ_{min} is not defined, it is set as the smallest eigenvalue of the set with all the candidate points.

4.3 Normalization of Torque

Another improvement is about the balance between the force and torque. The terms of “force” and “torque” come from the kinematic area; we borrow them for our geometric problem to describe the power that induces the corresponding translation along $\delta \mathbf{t}$ and rotation around $\delta \mathbf{r}$. The normalization actually depends on the nature of applications. For example, in a kinematic problem, the magnitude of torque depends on the position – the farther from the center a point is, the larger torque is needed for a rotation. However, ICP itself is a geometric problem, and thus normalization is needed to make the magnitudes of translations and rotations compatible to each other. It can be easily verified that ICP is scale-





									
		#point	time	#point	time	#point	time	#point	time
I		203	351	232	722	401	1224	146	832
L_{avg}	II	176	299	66	361	270	914	Same as I	
	III	88	195	54	239	194	493	64	376
L_{pn}	II	186	313	192	491	380	1170	120	594
	III	148	270	79	160	218	455	69	301
L_{max}	II	140	251	110	483	170	646	80	378
	III	32	116	40	213	134	458	56	290
$\frac{3}{2}L_{max}$	II	140	248	110	618	190	615	72	349
	III	30	178	34	340	122	706	66	339

Table 1. Comparison of the torque’s normalization methods. Cases I, II, and III are three different sets of points, which are detailed in the paragraph. #point gives the number of points, and time is the total time (in ms) for ICP to converge. The tests are run on a computer with 2GZ Dual-Core CPU.

independent. (One can run an ICP on a model and its scaled-down version, e.g., 10^{-4} times smaller, and the two results will be identical.) In this sense, torque does not match the nature of ICP, and it should be normalized with respect to the object’s size, i.e.,

$$\mathbf{u}_i = \left[\begin{array}{c} \mathbf{n}_i \\ \frac{1}{L} \mathbf{p}_i \times \mathbf{n}_i \end{array} \right]. \quad (6)$$

Notice that, as the stability analysis is fully based on the eigenvalues that are highly related to the magnitudes of force and torque, a correct normalization is crucial. The problem is how L should be set to give a correct normalization.

The most common practice [5, 24], and also what Gelfand et al. [6] did, is to set $L = L_{avg}$ as the average distance of the points from the center, so that the torque is scale-independent and the contribution of each torque is optimized. However, we can also set $L = L_{max}$ as the maximum distance (i.e., scale the object to be inscribed in a unit ball), or set $L = L_{pn} = \|\mathbf{p}_i \times \mathbf{n}_i\|$ to normalize the effect by the torque on each point. It is unknown yet which of them is better or the best. In this paper, we give a study and induce the best one particular for ICP. Recall that the stability analysis is to measure the energy introduced by a given force. It can also be seen as the response under a given force. For example, when a unit force is applied, the greatest response is that the point undergoes a unit translation along the force direction. It is similar in rotation. Although rotation is a bit more complicated as it is also related to the distance from the center, the maximum response can still be one. It makes no sense that a point can displace more than the torque induced. As a result, we deduce that $L = L_{max}$ is the desired normalization for ICP. In order to verify this conjecture, we use our framework to

evaluate the performances of different settings to check if the results match our study.

The experiment is set as follows. First (I), a set of arbitrary points that can successfully output the correct registration under ICP is chosen. Second (II), this set of points are input to our point extraction method, and the smallest eigenvalue is used as λ_{min} to find the minimum number of points among the set. The extracted points are then used to run ICP again. Third (III), the result is further verified by the feature points extracted with λ_{min} from all the points of the object. The best normalization method should be the one that gives the smallest number of feature points and can register correctly. The results of this experiment are shown in Table 1. Four normalization methods are tested, including L_{avg} , L_{pn} , L_{max} and $\frac{3}{2}L_{max}$, where the last one is used to check if the best solution is beyond L_{max} . We record the results by the number of points and the total computing time used in the ICP process until it is converged, with the termination condition set as the alignment error being smaller than $1e-5$. From the table, a few observations can be made:

1. L_{pn} gives the worst performance, because it always returns the largest number of points, and takes the longest time to converge.
2. L_{avg} is better than L_{pn} , but the numbers of the retained points in cases II and III are much larger than that from L_{max} .
3. $\frac{3}{2}L_{max}$ has the similar performance as L_{max} in terms of the number of points, but the computing time needed to converge is longer than that by L_{max} . This means that the extracted points tend to be less stable than those from L_{max} , and the iteration may be prone to divergence.

As a result, we find that the best performance for ICP is using L_{max} to normalize the torque, which agrees with our study.

5 Results

The stability analysis reports how much the given point set constrains different motions. The sampling framework discussed in this paper can be adaptive to the needs in stability. The higher the values are, the more stable the system is. Two test cases are shown in Fig.3. We demonstrate by a regular shape – a cube, and a featureless model – a blade. The black points are the candidate points for registration, and the red points are the selected points from the candidate points for different levels of stability. It shows that more points are needed for a higher stability. Meanwhile, the points are basically located as far as possible from the center, because those points contribute more to the torque – $\mathbf{p}_i \times \mathbf{n}_i$.

We also compare our improved algorithm with the original covariance sampling. In this comparison, we set the same required stability λ_{min} for both methods, and run ICP for the corresponding sampling results. The Root-Mean-Square (RMS) alignment errors are recorded in the iterations throughout, and they are plotted as charts in Fig.4. The alignment error measures the distances between a point in P and its projected position on S . We set $\lambda_{min} = 10$ in the experiments. For the rabbit example, all the ICP iterations till con-

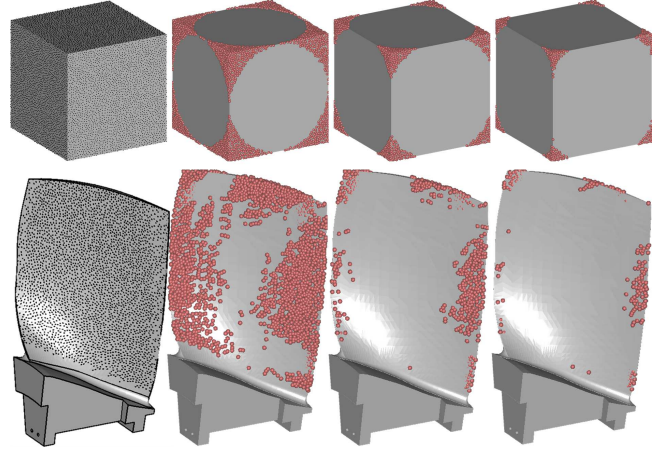


Fig. 3. Two examples of point extraction: a cube (top) and a blade (bottom). From left to right: the input, and three cases with different stabilities of 40.0, 20.0, and 10.0 for cube; 8.0, 4.0, 2.0 for blade. Black points are the candidate points, and red points are the extracted points.

vergence are shown. It can be seen that the improved method globally converges much faster than the original method. The improved method has already converged after about 80 iterations, while the original method takes more than 180 iterations to converge. A sharper comparison is shown in the rocker arm model. The improved method is converged after 120 iterations, but the original method needs around 260 iterations. In both examples, we can see that the convergence rate is increased more than 2 times in the improved version. The last example in Fig.4 is a chair model. It clearly shows that the original method fails to converge, but the improved method does. This is because the stability of the original method is not as accurate as the improved one, and thus the set of points is in fact not fulfilling the required stability, even though the original analysis falsely says so.

Beside the original stability analysis, we have also conducted some comparisons between our method and other popular point selection methods. Specifically, we compared with the Heat Kernel Signature (HKS) method [18], the 3D-SIFT method [8], and the Normal-Space Sampling (NSS) method [14], in Fig.5. Two real models are tested: a shoe and a screwdriver. In our tests, HKS is found to be unstable and also performs the worst (it cannot converge and keep vibrating). This is because it selects the points which are the local maxima of HKS, but there are not many such points in rough or noisy models. NSS is better; but since it in general ignores the shape of the model, its convergence is slow or even diverges. 3D-SIFT can successfully converge, but it is much slower when compared with our method.

6 Conclusion

The Iterative Closest Point (ICP) algorithm is a widely used method for registration of three-dimensional point sets. The quality of registration obtained by this algorithm depends heavily on choosing good pairs of corresponding

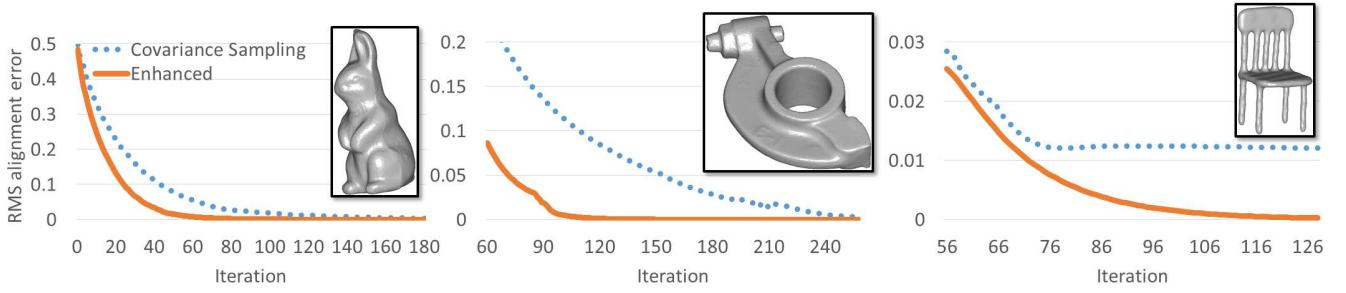


Fig. 4. Comparison between the original covariance sampling and the improved one proposed in this paper. Three examples are shown in this figure, and each of them shows a chart of Root-Mean-Square (RMS) alignment error against the iteration steps. From the rabbit and rocker arm examples, we can see that the improved version converges more than 2 times faster than the original one. In the chair example, even though both methods have the same minimum stability, the original method fails to converge while the improved one does.

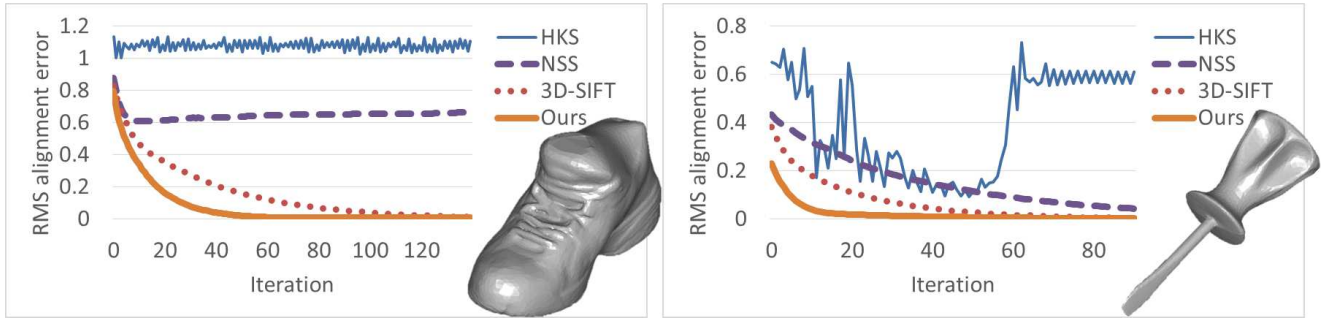


Fig. 5. Comparisons between our method and the Heat Kernel Signature (HKS) method, the Normal-Space Sampling (NSS) method, and the 3D-SIFT method. In the tests on both objects, our method performs much better than the rest.

points in the two datasets. The stability analysis proposed by Gelfand et al. [6], which makes use of the covariance to study the effect between its eigenvalues and the convergence of ICP, provides a good means for this point selection task. To have an accurate analysis result, we have proposed several improvements in this paper. First, we have developed a two-phase iteration algorithm to solve the nonlinear optimization problem due to finding the correct rotation center. Second, another nonlinear optimization problem in point extraction is solved by another two-phase algorithm through iterative addition and reduction of the selected points. Finally, through experiments we have shown that a correct normalization between the torque and force is not to resize the model to make its average length (from the center) to be one; instead, it should be scaled to be inscribed in a unit ball. Our experimental results show a great improvement in terms of efficiency and robustness after these improvements have been made.

There are some limitations of the proposed approach. First, the analysis works well in complete scans; however, when the range surfaces are overlapped only partially (see Fig.6 for an illustration), the analysis can only be done on the overlapping parts, which means that the analysis has to be re-done for every pair of the surfaces. Second, the proposed approach may suffer from high levels of noise, as large noises make some originally smooth areas strongly constraining. The noise could be introduced by the inaccuracy of hardware setup, background color or light for vision scanning device, or vibration in operation. To illustrate the problem, an ex-

ample of a teapot is shown in Fig.7, in which different levels of noise are added for comparison. We distribute Gaussian noise on the vertices in the normal direction, and the amount of noise is specified by a percentage of the model's bounding ball radius. As it is no longer fair to measure the alignment error directly in the object space for a model with noise, we measure the transformation error, which is the difference between the computed transformation matrix at each step and the desired transformation matrix. The desired transformation matrix is known because the motion of the model from its original position is known, and we use Frobenius norm (i.e., the matrix norm) to compute the difference. It can be seen that with the level of noise increased, the transformation error cannot converge to zero. These two issues will be studied in the future.

Acknowledgement

This project is supported by the Hong Kong ITF GHP/057/12.

References

- [1] P. J. Besl and N. D. McKay. A method for registration of 3-D shapes. *IEEE Trans. Pattern Anal. Mach. Intell.*, 14(2):239–256, Feb. 1992.
- [2] M. Bokeloh, A. Berner, M. Wand, H.-P. Seidel, and A. Schilling. Slippage features, 2008.
- [3] Y. Chen and G. Medioni. Object modelling by registra-

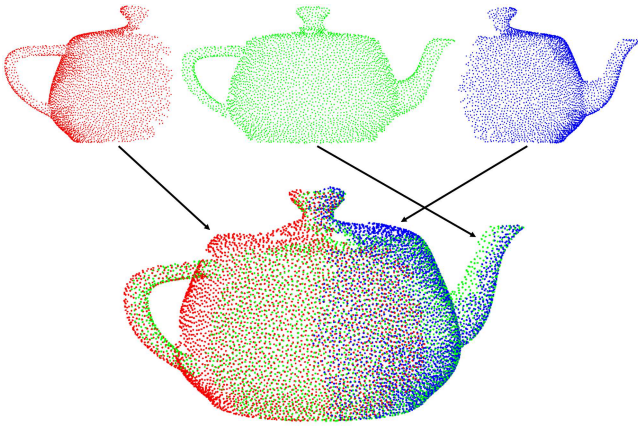


Fig. 6. Three range surfaces capture different portions of a teapot, and their data are overlapped only partially.

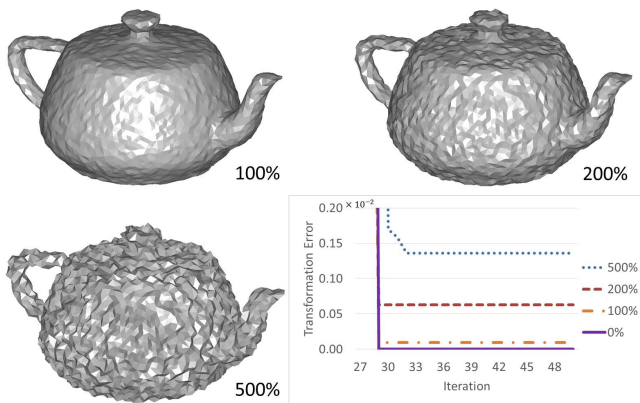


Fig. 7. Comparison between different levels of Gaussian noise is added in terms of transformation error. The amount of noise is related to the percentage of the model's bounding ball radius.

tion of multiple range images. *Image Vision Comput.*, 10(3):145–155, Apr. 1992.

- [4] T. Gatzke, C. Grimm, M. Garland, and S. Zelinka. Curvature maps for local shape comparison. In *Proceedings of the International Conference on Shape Modeling and Applications*, SMI '05, pages 246–255, 2005.
- [5] N. Gelfand and L. J. Guibas. Shape segmentation using local slippage analysis. In *Proceedings of the Eurographics/ACM SIGGRAPH Symposium on Geometry Processing*, SGP '04, pages 214–223, 2004.
- [6] N. Gelfand, L. Ikemoto, S. Rusinkiewicz, and M. Levoy. Geometrically stable sampling for the ICP algorithm. In *Proceedings. Fourth International Conference on 3-D Digital Imaging and Modeling (3DIM)*, pages 260–267, Oct 2003.
- [7] N. Gelfand, N. J. Mitra, L. J. Guibas, and H. Pottmann. Robust global registration. In *Proceedings of the Third Eurographics Symposium on Geometry Processing*, SGP '05, 2005.
- [8] A. Godil and A. I. Wagan. Salient local 3d features for 3d shape retrieval. volume 7864, pages 78640S–78640S–8, 2011.
- [9] P. Heider, A. Pierre-Pierre, R. Li, and C. Grimm. Local shape descriptors, a survey and evaluation. In *Proceedings of the 4th Eurographics Conference on 3D Object Retrieval*, EG 3DOR'11, pages 49–56, 2011.
- [10] T.-H. Kwok, K.-Y. Yeung, and C. C. L. Wang. Volumetric template fitting for human body reconstruction from incomplete data. *Journal of Manufacturing Systems*, 33(4):678 – 689, 2014.
- [11] T. Masuda, K. Sakaue, and N. Yokoya. Registration and integration of multiple range images for 3-D model construction. In *Proceedings of the 13th International Conference on Pattern Recognition*, volume 1, pages 879–883, Aug 1996.
- [12] N. J. Mitra, N. Gelfand, H. Pottmann, and L. Guibas. Registration of point cloud data from a geometric optimization perspective. In *Proceedings of the Eurographics/ACM SIGGRAPH Symposium on Geometry Processing*, SGP '04, pages 22–31, 2004.
- [13] H. Pottmann and S. Leopoldsdeder. A concept for parametric surface fitting which avoids the parametrization problem. *Computer Aided Geometric Design*, 20(6):343–362, sep 2003.
- [14] S. Rusinkiewicz and M. Levoy. Efficient variants of the ICP algorithm. In *Third International Conference on 3D Digital Imaging and Modeling (3DIM)*, June 2001.
- [15] J. Salvi, C. Matabosch, D. Fofi, and J. Forest. A review of recent range image registration methods with accuracy evaluation. *Image Vision Comput.*, 25(5):578–596, May 2007.
- [16] R. Song, Y. Liu, R. R. Martin, and P. L. Rosin. Saliency-guided integration of multiple scans. In *IEEE Conference on Computer Vision and Pattern Recognition (CVPR)*, pages 1474–1481, June 2012.
- [17] X. Song, Y. Pan, and Y. Chen. Development of a low-cost parallel kinematic machine for multidirectional additive manufacturing. *J. Manuf. Sci. Eng.*, 137(2):021005, 2015.
- [18] J. Sun, M. Ovsjanikov, and L. Guibas. A concise and provably informative multi-scale signature based on heat diffusion. In *Proceedings of the Symposium on Geometry Processing*, pages 1383–1392, 2009.
- [19] A. Tevs, A. Berner, M. Wand, I. Ihrke, and H.-P. Seidel. Intrinsic shape matching by planned landmark sampling. volume 30, pages 543–552, 2011.
- [20] G. Turk and M. Levoy. Zippered polygon meshes from range images. In *Proceedings of the 21st Annual Conference on Computer Graphics and Interactive Techniques*, SIGGRAPH '94, pages 311–318, 1994.
- [21] W. Wang, H. Pottmann, and Y. Liu. Fitting b-spline curves to point clouds by curvature-based squared distance minimization. *ACM Trans. Graph.*, 25(2):214–238, Apr. 2006.
- [22] S. Weik. Registration of 3-D partial surface models using luminance and depth information. In *Proceedings of International Conference on Recent Advances in 3-D Digital Imaging and Modeling*, pages 93–100, May 1997.
- [23] K. Xu and Y. Chen. Mask image planning for deforma-

tion control in projection-based stereolithography process. *J. Manuf. Sci. Eng.*, 137(3):031014, 2015.

- [24] Y. Zheng, M. C. Lin, and D. Manocha. Efficient simplex computation for fixture layout design. *Computer-Aided Design*, 43(10):1307 – 1318, 2011.